Experimental Investigation of a 7 by 7 Nozzle Jet Array for Dynamic Impingement Cooling

Frank Haucke, Henning Kroll, Inken Peltzer and Wolfgang Nitsche

Technische Universität Berlin, Department of Aeronautics and Astronautics, Chair of Aerodynamics,
Marchstr. 12-14, 10587 Berlin, Germany
{Frank.Haucke,Henning.Kroll,Wolfgang.Nitsche}@ilr.tu-berlin.de
Inken.Peltzer@tu-berlin.de

Abstract. Dynamic impingement cooling is a promising way for more efficient exploitation of cooling air in highly heat charged environments. In many applications the deployed impinging jets are subjected to cross flow superimposed on the flow field of the transverse jets. The present study describes the initial experimental investigations regarding dynamic heat transfer between a flat surface and an array of 49 impingement jets, which are dynamically controlled by changing frequency, duty cycle and phasing. A new test rig was designed and manufactured in order to investigate the interactions of impingement jets and their impact on heat transfer. The test rig satisfies the needs of different measurement techniques. Surface measurements using pressure sensors, thermocouples, hot wires, hot films and liquid crystal thermography are planned for investigating the interactions near the wall. Furthermore, the test rig is suitable for efficient flow field measurements between jet orifices and impingement plate using particle image velocimetry. Parallel to the test rig development, time resolved PIV measurements have been performed in the test section of a recirculating free-surface water tunnel in order to investigate the influence of cross flow superimposed to periodically generated vortex rings impinging on a flat plate. The central goal of these preliminary testing is to understand under which formation conditions periodically generated vortex rings in cross flow have the ability to maximize the transport of vorticity close to the wall. First results are presented and discussed.

Keywords: Impingement cooling, dynamic forcing, heat transfer, vortex rings, crossflow

1 Introduction

Since turbine inlet temperatures were increased, the effectiveness of the thermodynamic cycle could be enhanced significantly. Thereby the tolerable specific material temperatures were exceeded, which made it mandatory to develop effective cooling strategies inside turbo machinery since 1960. Modern Trent engines

have a turbine inlet temperature of about 1700K [13]. Only specific turbine materials in combination with a sophisticated cooling strategy make it possible to operate engine components above their temperature limits. An increased efficiency of the thermodynamic cycle, as a result of high operating temperatures, has to be paid with cooling air bypassed from the high pressure compressor of the same engine. All air that has to be extracted from the "cold" primary air stream reduces the efficiency of the gas turbine cycle and is therefore expensive. In order to reduce the consumption of bypass air, the cooling strategy for hot components has to become more efficient. Investigations are focused on the interaction between impinging jets and surfaces [1], [2], [3], [4]. Pagenkopf [8] provides a chronological overview of standard impingement cooling using steady jets. A promising way for enhancing heat transfer can be achieved by means of excited impingement jets. A theoretic approach to pulsating impingement jets was desired by Zumbrunnen [9]. An analytic model was developed to determine the transient response characteristics of the thermal boundary layer. Regarding heat transfer enhancements, Zumbrunnen and Aziz [10] derived a minimum Strouhal number for jet excitation. Using Strouhal numbers above $Sr_D = 0.26$ leads to higher time averaged wall heat fluxes due to higher temperature gradients inside the thermal boundary layer of the wall. Strouhal numbers lower than $Sr_D = 0.26$ can cause reductions in heat transfer of about 17%, which was detected by Sheriff and Zumbrunnen [11]. The same authors achieved heat transfer enhancements of up to 33% for Strouhal numbers of up to $Sr \leq 0.51$. Janetzke et al. [5], [6], [7] investigated experimentally the local flow field of impinging jets of a 3-nozzle-line-array and its impact on the local wall heat flux of a steam heated impingement plate. There, the nozzle Reynolds number was varied up to $Re_D = 7880$. During dynamic measurements all nozzle jets were excited in phase with corresponding Strouhal numbers of up to $Sr_D \leq 0.97$. Compared to Zummbrunnen's theoretical threshold Strouhal number of $Sr_D = 0.26$, Janetzke experimentally found a corresponding Strouhal number of $Sr_D = 0.28$ for high amplitudes. For low amplitudes this threshold Strouhal number is shifted to $Sr_D = 0.6$, see Fig. 1. This means beside the excitation Strouhal number the excitation amplitude plays an immense role for increasing heat transfer. Furthermore fluid mechanical analysis of the flow field using particle image velocimetry was conducted for the same range of excitation parameters. Due to pulsation, phase triggered periodic velocity maxima were generated. This dynamic forcing, using Strouhal numbers larger than $Sr > 0.3$, affected the shear layer around each impingement jet and triggered the in-phase propagation of large toroidal vortices. The response characteristics of the toroidal vortices on the excitation can explain the mechanism of heat transfer enhancements, compared to steady conditions. Depending on Strouhal number and amplitude, weak or strong circular vortex structures around each impingement jet will be generated. Thus, using the appropriate excitation parameters can force renewal effects of the velocity and thermal boundary layer, which lead to the heat transfer enhancements.

Based on the results of Janetzke et al. [5], [6], [7], this work will extend the findings for 3-nozzle-line-array to a 7 by 7 nozzle array. Although the geometri-

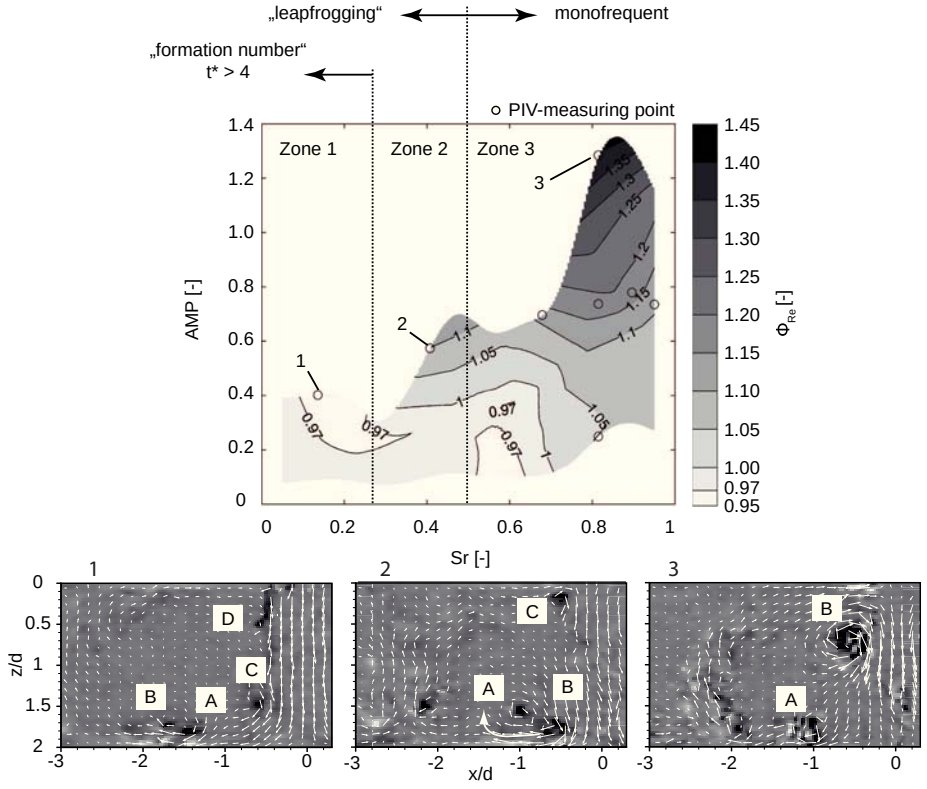

Fig. 1. Stagnation point cooling effectiveness and corresponding velocity vector field of impingement jets. Janetzke [7].

cal dimensions of generic experimental set-ups for impingement cooling are still large, compared to engine applications, understanding the mechanisms of heat transfer between hot surfaces and dynamic coolant jet arrays inside hot casings is key for the development of new efficient cooling strategies. In addition, the preliminary tests define a first approach to study the flow topology employed by periodically generated vortex rings in a cross flow environment. Beyond that, the preliminary study focuses on the investigation of the segregated impact of frequency, duty cycle and corresponding stroke ratio on cooling efficiency, quantified by the vorticity field in the near wall region.

2 Preliminary study

Impinging jets, deployed in applications involving impingement cooling configurations, are in many cases subjected to cross flow superimposed on the flow field of the transverse jet. Preliminary tests have been carried out in order to investigate the influence of cross flow superimposed to periodically generated

vortex rings impinging on a flat plate. The connection between enhanced heat transfer and the interaction of large-scale vortices in the vicinity of thermally loaded surfaces is well known (Kataoka et al.[14]). Thus approaches concerning the optimization of impingement cooling systems require a detailed knowledge about the flow topology, particularly in the near wall region. Local heat transfer is to a large extend connected to the wall-bounded velocity gradient. Hence the central goal of the preliminary tests is to understand under which formation conditions periodically generated vortex rings have the ability to maximize the transport of vorticity close to the wall. For a given velocity ratio $VR = U_{jet}/U_\infty$, the governing parameters are the non-dimensional form of pulsation frequency $Sr_D = f \cdot D/U_{jet}$ and the duty cycle $DC = \tau/T$. Herein τ refers to the temporal pulse width and $T = 1/f$ represents the periodic time. In terms of vortex ring formation, there is another key parameter namely the stroke ratio L/D, the non dimensional form of the slug length L ejected from a commonly used piston-cylinder arrangement for vortex ring generation. In case of fully modulated pulsation as described by Sau and Mahesh [15], this set of parameters is linked via the following equation:

$$DC = \frac{L}{D} \cdot Sr_D$$

In terms of flow topology, the three parameters can be interpreted as follows:

- $\mathbf{Sr_D}$: Determines the spacing of generated vortices, causing different interactions between individual vortex cores
- **L/D**: Determines if vortex rings are generated with or without trailing column. Moreover, the stroke ratio correlates with the intensity of individual vortices in terms of their level of circulation (Gharib et al.[16])
- **DC**: Affects the spatial arrangement between the trailing column (if present) of leading vortices and the following vortex ring. In addition, the duty cycle is directly related to the ejected mass flux

The preliminary study focuses on the segregated impact of these three parameters on cooling efficiency, quantified by the vorticity field in the near wall region. The dependency of the individual parameters infers that there are only two independent parameters governing the problem. Taking Sr_D and L/D as the two independent variables from the expression $DC = \frac{L}{D} \cdot Sr_D$ suggests that the aforementioned separate effects are dominant in that issue.

Time resolved PIV measurements have been performed, providing a unique opportunity to analyse transient flow structures and representing a powerful tool to allow inspection of the key features of the flow. The measurements were carried out in the test section of a recirculating free-surface water tunnel, displayed in Fig. 2(a). The tunnel was running at constant flow velocity $U_\infty = 11.1cm/s$ and the turbulence intensity in the test section was measured at about 1%. Three independent vortex rings were generated by a piston-cylinder arrangement in conjunction with a nozzle, providing a contraction ratio of 1:2 and an exit diameter of $D = 1.3cm$. The nozzle exit plane was mounted flush with the

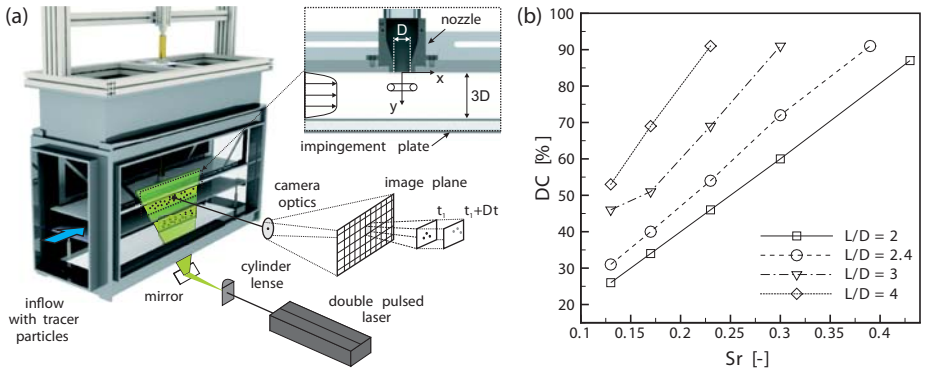

Fig. 2. Assembly and test section of water channel (a) and range of tested parameters at fixed velocity ratio $VR = 4.3$ (b)

surface of a ceiling plate, $57.2cm$ downstream of the leading edge of the plate. An impingement plate was mounted parallel to the ceiling plate, with a fixed plate clearance of $3D$. Each vortex ring was generated at constant mean jet velocity $U_{jet} = 48.5cm/s$ by means of time-averaging over the pulse width τ. The corresponding velocity ratio and Reynolds number are $VR = 4.3$ and $Re_D = 6300$ respectively. The range of measured parameters is shown in Fig. 2(b). Depending on the stroke ratio L/D, the maxima of acquirable frequencies are restricted by the output power of the electro-mechanical drive of the piston. As indicated by the Fig., the set of tested parameters allows comparisons at fixed values of each individual parameter.

Frequency: Fig. 3 shows the influence of pulsation frequency on the overall flow topology at the same instant of non dimensional time $t^* = t \cdot U_{jet}/D = 6.64$, corresponding to the moment of impact on the impingement plate of the first generated vortex. The cores of the vortex rings are numbered consecutively with respect to their sequential arrangement.

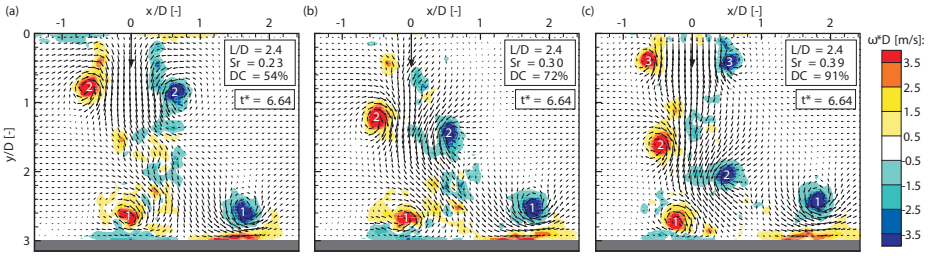

Fig. 3. Flow topology at $t^* = 6.64$. $VR = 4.3$, $L/D = 2.4$ and (a): $Sr_D = 0.23$; (b): $Sr_D = 0.30$; (c): $Sr_D = 0.39$

Higher frequencies yield closer vortex spacing and thus stronger interactions between the individual vortex cores. If the spacing is reduced, the second vortex ring (No.2) encounters a tilting mechanism caused by the induced velocity field of the surrounding vortices. In this case, the alteration of the spacial arrangement affects the impact positions of the vortices on the impingement plate. In the near wall region the vorticity of opposite sign induced by the first vortex elements is evident in all cases. The vorticity field indicates locally strong velocity gradients at the wall and thus potentially high local heat transfer rates. In Fig. 4 the absolute value of vorticity next to the wall $|\omega|_y$ is diagrammed over the wall coordinate x/D and over time.

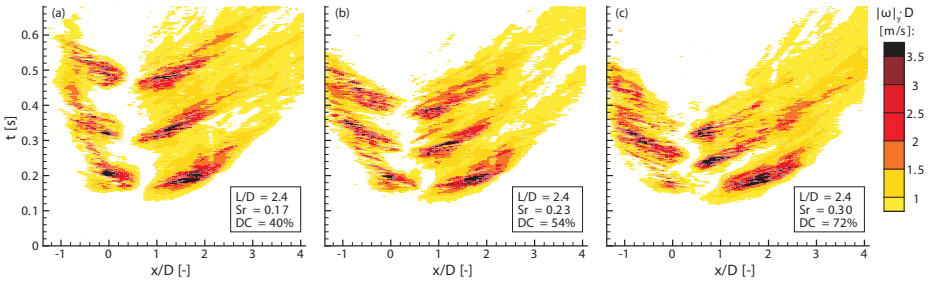

Fig. 4. Absolute vorticity $|\omega|_y \cdot D$ next to the wall. $VR = 4.3$, $L/D = 2.4$ and (a): $Sr_D = 0.17$; (b): $Sr_D = 0.23$; (c): $Sr_D = 0.30$

The coloured contours can be interpreted as the temporal and spatial arrangement of the impact events of the vortices on the wall, herein after referred to as *footprints*. As the frequency is increased, the footprints move closer together on both counts, temporally and spacial due to the aforementioned tilting mechanism of subsequent vortices.

Stroke ratio: In Fig. 5 the influence of the stroke ratio on the flow topology at constant phase $\phi/2\pi = 2.02$ is depicted, corresponding to the beginning of generation of vortex no.3.

Meanwhile in both cases $L/D = 2$ and $L/D = 4$, the first vortex causes a boundary layer renewal process and the formation of a secondary vortex. The development of the secondary vortex indicates separation of the boundary layer from the wall and restricts the area influenced by the vortex element on the plate. In contrast to the case $L/D = 2$, vortices generated with $L/D = 4$, as indicated in Fig. 5(b), involve the development of a distinct trailing column. This implies in turn that the vortices are saturated with respect to their ability to entrain vorticity from the ejected shear layer and hence their level of circulation. Vortex rings generated in a quiescent fluid attain maximum circulation, if the stroke ratio is in the order of the *formation number* ($f\# \approx 3.6$), defined by Gharib et al. in [16]. However, if cross flow is imposed to the vortex rings,

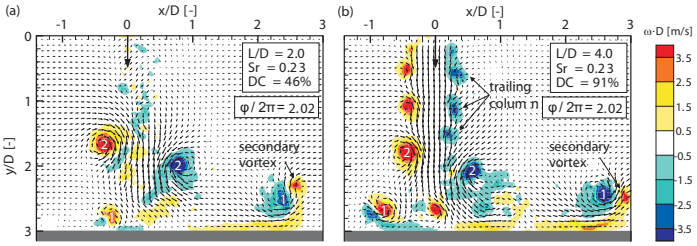

Fig. 5. Flow topology at constant phase $\phi/2\pi = 2.02$. $VR = 4.3$, $Sr_D = 0.23$ and (a): $L/D = 2.0$ (b): $L/D = 4.0$

entrainment of cross flow fluid occurs, especially on the lee-side of the vortex ring. As a consequence, the vortices pinch off the shear layer and are no longer gaining vorticity, restricting the circulation enhancement. The critical stroke ratio that separates vortex rings in cross flow with or without the development of a trailing column is referred to as *transition stroke ratio* $L/D_{tr} = f(VR)$, which is a function of velocity ratio and was specified by Sau and Mahesh in [17]. With increasing velocity ratio L/D_{tr} increases and approaches the formation number for $VR \to \infty$. Sau and Mahesh curve fit an exponential function through their data points of L/D_{tr}, and obtain $L/D_{tr}(VR = 4.3) = 2.9$, concerning the velocity ratio being investigated in the present study. Fig. 6 shows the footprints of the vortices on the surface of the plate at $Sr_D = 0.17$ obtained for $L/D = 2.4$ and $L/D = 4.0$.

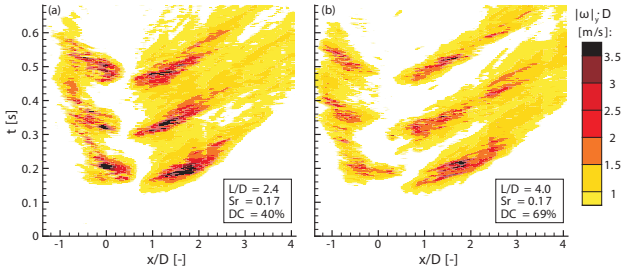

Fig. 6. Absolute vorticity $|\omega|_y \cdot D$ next to the wall. $VR = 4.3$, $Sr_D = 0.17$ and (a): $L/D = 2.4$; (b): $L/D = 4.0$

It is obvious that $L/D = 4.0$ yields significantly lower values of vorticity next to the wall compared to $L/D = 2.4$. This is due to the interaction of the vortices with the generated trailing column, which is being pushed between the plate and the leading vortex elements and attenuates vorticity transfer from the vortex to the boundary layer at the wall.

Duty cycle: The relationship of the parameters given by the expression $DC = \frac{L}{D} \cdot Sr_D$ implies that duty cycle is either changed by altering the stroke ratio or the frequency. Since the flow features are considered to be governed by the parameters Sr_D and L/D, the superior effect of duty cycle variation in this study is the related mass flux ejected from the nozzle into the cross flow. In this context, the duty cycle is used in order to attain a global measure of actual cooling power with respect to the applied mass flux. By averaging the absolute vorticity $|\omega|_y$ over the plate coordinate x/D and relating to DC and to the time interval Δt, which incorporates three cycle durations, one obtains

$$\Omega \equiv \frac{1}{DC \cdot \Delta t} \int_{t_0}^{t_0+3T} < |\omega|_y \cdot D >_x \, dt$$

In Fig. 7, Ω is depicted for the hole range of parameters tested. Single combinations of parameters are indicated by grey crosses in the same figure. An optimum can be found at $L/D = 2.4$ and $Sr_D = 0.3$. This combination is considered to provide a well-balanced relation between the vortex circulation, vortex spacing and applied mass flux.

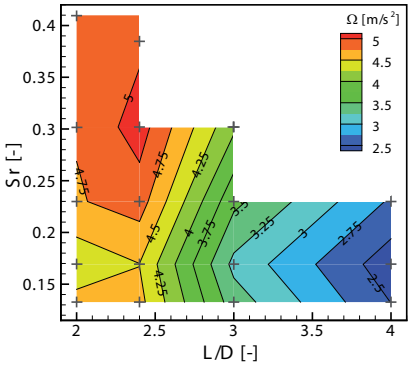

Fig. 7. Global measure of cooling efficiency Ω. $VR = 4.3$.

The stroke ratio is close to L/D_{tr} and corresponds to more or less saturated vortices without a trailing column. Possible higher local values of near wall vorticity in case of larger stroke ratios have to be paid with an increased mass flux, at the expense of cooling power. Lower stroke ratios yield less intense vortices and thus decreasing values of Ω. If L/D is kept constant, it is conceivable that higher frequencies cause unfavourable interactions due to reduced spacing of the vortex elements, in addition to an increased mass flux.

The findings of the preliminary study are reserved to prospective investigations and serve as guidelines referring to the pre selection of parameters in the optimization process.

3 Experimental setup

This work aims at investigation the interactions of a 7 by 7 impinging jet array in the presence of a flat surface. Here, nozzle design, nozzle to nozzle arrangement and impingement distance are important geometrical parameters, which need to be varied. Dynamic parameters such as coolant mass flow, pulse frequency, pulse duty cycle or phasing also need to be focused on. Considering an efficient variation of the mentioned parameters as well as the needs of standard aerodynamic measurement techniques, a test rig for investigating impingement cooling was designed. Fig. 8 shows the experimental set-up. 49 air nozzles are integrated within a horizontal flat aluminium plate. The main nozzle's dimensions are equivalent to those of Janetzke [5], which were used in a 3-nozzle-line-array. Within this work a 7 by 7-nozzle-array is employed. The normalized spacing between two nozzles is y/D=5. The nozzle geometry is equivalent to a simple drill hole using a diameter of D=12mm and using a length over diameter ratio of l/D=2.5. These values were taken from the work of Janetzke [5] as initial values for the upcoming experimental investigation in the framework of this project. The central component of this test rig is the impingement plate with the dimensions of 1m by 1m. Depending on the current measurement technique this plate can be easily replaced. For surface pressure measurements an aluminium plate is used. 289 wall pressure probes are integrated in a space of 800mm by 800mm. The spacing between two probes is 50mm. In order to achieve a high planar resolution of wall pressure distribution the impingement plate as well as the nozzle plate are moveable by computer controlled stepping motors, each plate in one horizontal direction. Furthermore, the nozzle to plate spacing z can be varied automatically as well, which allows set-up variations without altering the rig.

The air mass flow, which passes through each nozzle is supplied by a standard in-house compressed air system. In order to provide the desired amount of air, four mass flow control units are used. Each unit consists of an electronic proportional pressure regulator and an electronic mass flow controller, see Fig. 9. Both components are connected in series. In case of providing a constant amount of air, the electronic mass flow controller is used. The pressure regulator supplies the best working pressure for the mass flow controller. In specific cases it is possible to change the mass flow controller in gauging mode. Then, the electronic pressure regulator is used to set-up the mass flow by changing the working pressure much faster. Downstream of these components, one air flow divider is connected to each mass flow control unit and feeds up to 13 nozzles.

In case of investigating pulsed impingement jets, one fast switching valve unit is added before the compressed air is passed into each nozzle. These valve units are a modified version of the "MHJ9 valve series", produced by the FESTO company. The standard valve parameters are as follows: The normalized volume

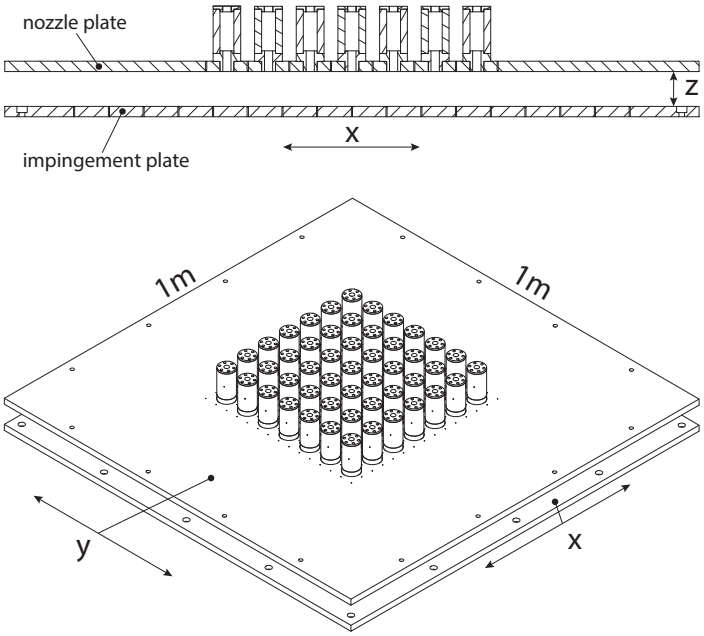

Fig. 8. Nozzle plate and impingement plate

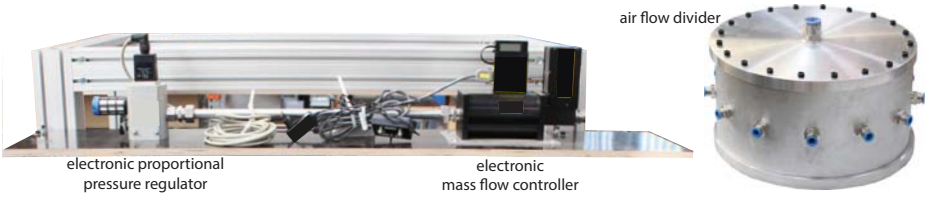

Fig. 9. Mass flow control unit and air flow divider.

flow rate is $V_N = 160 l_N/min$ and maximum switching frequency is $f_{e,max} = 500 Hz$. Two standard MHJ9-valves are used for one valve unit, see Fig. 10

Fig. 11 presents the test rig with the most important components. The mass flow control units are integrated on top of the test rig and feed the air flow divider below. Flexible tubes are employed to connect the air flow divider with the corresponding valve units or nozzles, respectively.

First experimental investigations were conducted to verify the quality of the 49 escaping nozzle jets without the presence of the impingement plate. At this point, a rake of seven Pitot tubes was used to determine the distribution of total pressure at the outlet area of each nozzle. This rake can be moved relative to

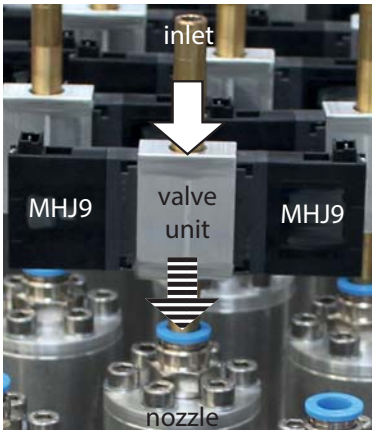

Fig. 10. Valve unit.

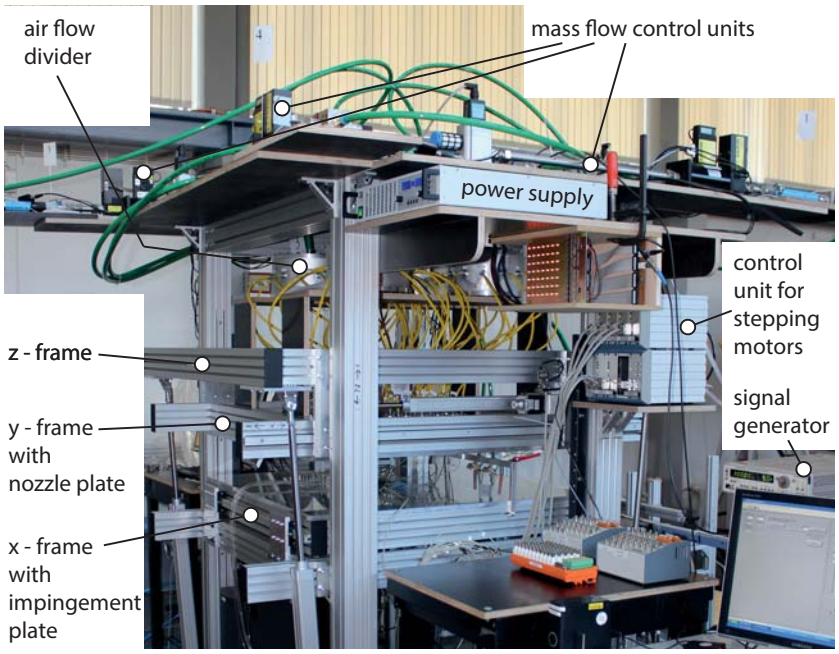

Fig. 11. Test rig for impingement cooling.

the nozzle plate in the same way as the impingement plate. As a result, the distribution of the absolute velocity at the nozzle outlet indicates if all nozzles will work in the same way.

The presented test rig is also prepared for optical measurement techniques that will be carried out later in the project. A good optical accessibility to the

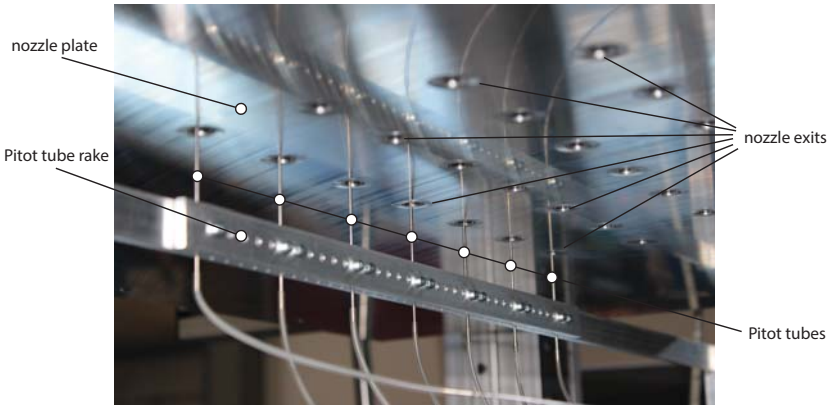

Fig. 12. Pitot tube rake.

impingement plate and to the flow field of the jets is a very important requirement, which was considered during the design of the test rig. The aluminium impingement plate can easily be exchanged for a glass plate. This allows an optical access from the bottom, through the glass plate and into the flow area. Thus, oil flow visualizations or liquid crystal thermography can be conducted with a minimum of optical blockage. Furthermore, investigating the flow field by using particle image velocimetry is another important goal of this project. Therefore, the optical accessibility from all four horizontal sides is given. It is possible to use a fixed stereoscopic camera to laser sheet arrangement while the nozzle array can be moved stepwise through the laser light sheet by moving the nozzle plate. The stereoscopic camera set-up allows the determination of the three spatial velocity components in a two-dimensional plane ("2D-3C") perpendicular to the impingement plate. By moving the nozzle plate the laser light sheet can be repositioned relative to the nozzles without changing any camera or laser light sheet adjustments, which is an immense benefit for efficient measuring. In the post process the "2D-3C"-velocity fields, obtained for each measurement plane, will be defragmented to a "3D-3C" volume area where all three spatial velocity components are known. This allows a very detailed experimental investigation of the interactions of the impingement jet array.

4 Experimental results and discussion

Up until now, only experimental investigations for isothermal conditions were conducted. The equality of the impingement jets at each outlet was verified for steady blowing without the presence of the impingement plate. The distribution of the static wall pressure was investigated as well in order to determine an absolute velocity field near the wall. Figure 13 shows first velocity data measured in the outlet plane of the nozzles for steady blowing conditions. This test was used to verify that all nozzles deliver almost equivalent outflow. The calculated

normalized volume flow rate is 58.33 l_N/min per nozzle, which corresponds to a diameter based Reynolds number of $Re_D = 6800$. The jet velocity within the core can differ from nozzle to nozzle by up to 7% which is satisfactory.

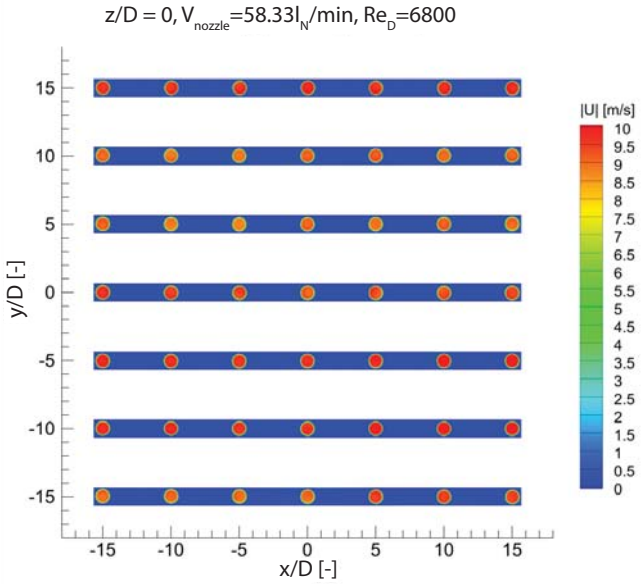

Fig. 13. Distribution of nozzle exit velocity with steady blowing.

Figure 14 shows the velocity profile along the line $y/D = z/D = 0$ for steady blowing. This result indicates that the maximum velocity level is equivalent at each nozzle for each presented nozzle Reynolds number. This is the prerequisite for further investigations in presence of the impingement plate.

In preparation for experimental investigations with heat transfer, the influence of the jet-array on the impingement plate is of special interest. At first, no heat transfer is considered. The absolute velocity distribution near the wall was determined by measuring the local static pressure distribution on the impingement plate. Figure 15 shows the corresponding result for an impingement distance of $z/D = 0.33$ and a nozzle Reynolds number of $Re_D = 6344$. External cross flow was not present. Primarily, a very symmetric flow field near the wall was detected, which indicates that all jets are almost equal. In theory, using a 7 by 7 jet array 49 stagnation regions on the impingement plate can be expected. In this specific case the absolute flow velocity is decelerated to 0 m/s only in the impingement area of the centre nozzle. The measurements indicate that the velocity level of the adjacent impingement regions is only close to 0 m/s. For increasing lateral distance to the centre nozzle the velocity level is increased as well. Thereby, in the peripheral area of the jet array no stagnation zones can be detected on the impingement plate.

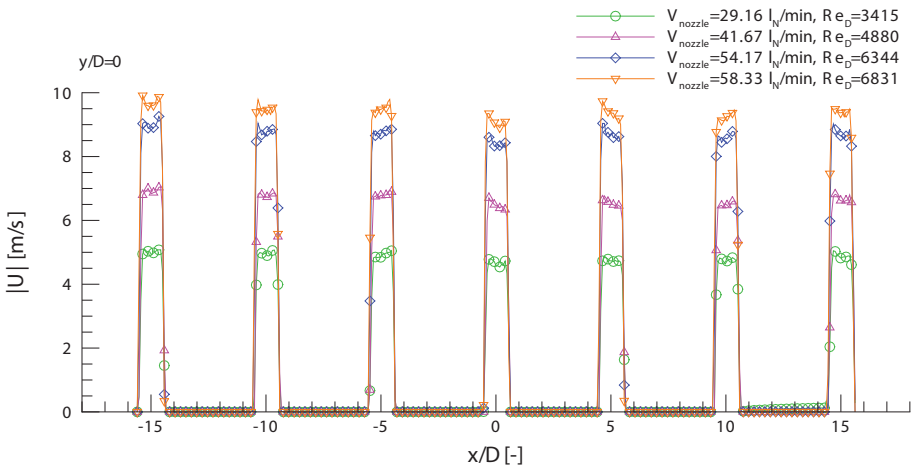

Fig. 14. Profiles of nozzle exit velocity at y/D=0 for steady blowing.

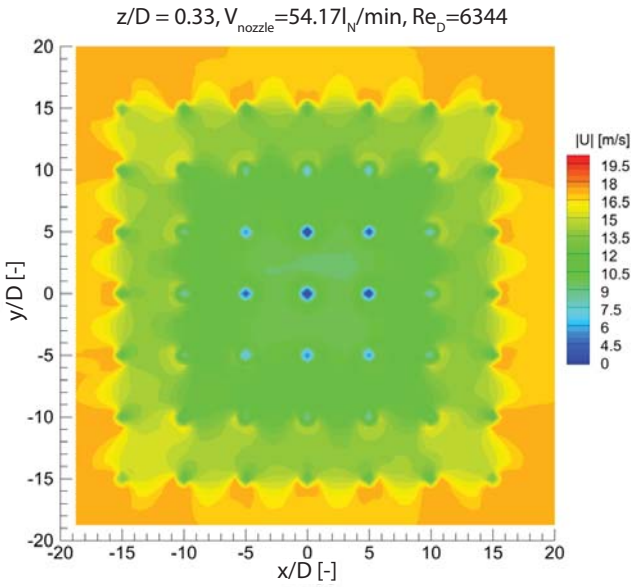

Fig. 15. Distribution of absolute velocity near the impingement plate with steady blowing.

In the left plot of Fig. 16 the absolute velocity profiles at $y/D = 0$ and $z/D = 0.33$ are plotted for different impingement distances and a constant nozzle Reynolds number of $Re_D = 6344$. In all presented cases the flow velocity

accelerates laterally from inside towards outside of the impingement plate. The location of each jet axis is clearly detectable every $\Delta x/D = 5$ steps where the velocity level is reduced significantly. Only for the 3 by 3 centre nozzles the flow velocity within the corresponding impingement jets near the wall is equal or close to 0 m/s. Obviously, a cross flow component is induced by the impingement jets which directly depends on the impingement distance. The smaller the distance between nozzle plate and impingement plate the higher the self induced cross flow, especially in the peripheral area of the set-up. A similar behaviour can be observed for a variation of nozzle Reynolds number and constant distance between the two counter plates, which is shown in the right plot of Fig. 16.

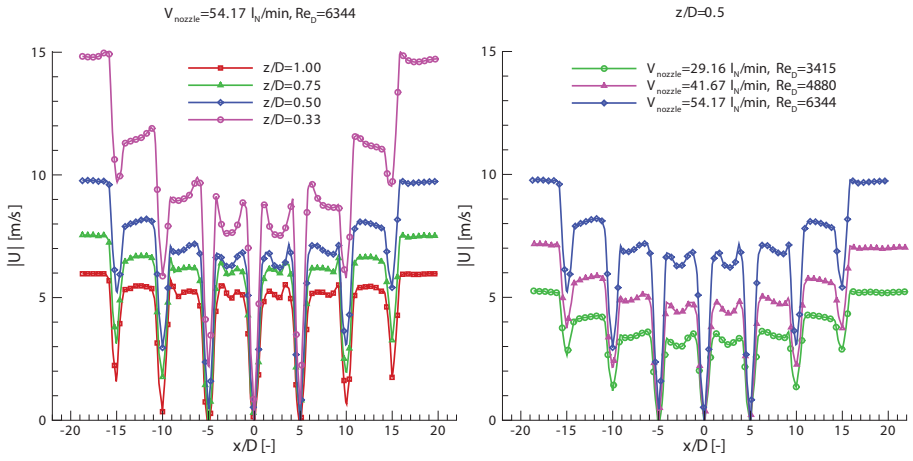

Fig. 16. Profiles of absolute velocity near the impingement plate at y/D=0 with steady blowing.

5 Conclusion

A new test rig for experimental investigations of dynamic impingement cooling was designed and manufactured. The impact of a 7 by 7 impingement jet array on the heat transfer on an impingement plate will be investigated. Many parameters have to be taken into account during the forthcoming experimental investigations. Among others the following parameters have significant impact on heat transfer and will be varied:

- nozzle jet arrangement
- nozzle geometry
- impingement distance
- coolant mass flow
- pulse frequency

– pulse duty cycle
– phase shift of excitation of adjacent nozzle jets

Pressure probes, hot wires, hot films, thermocouples etc. will be employed for standard investigations. Furthermore, the test rig is prepared for specific measurement techniques, such as stereoscopic particle image velocimetry and liquid crystal thermography. This work presents first data, which has been obtained during the verification of the nozzle jet array. A Pitot tube rake was used to determine the absolute velocity profiles at each nozzle outlet for steady blowing conditions and without the presence of the impingement plate. The characteristics of each nozzle jet are almost identical under different nozzle Reynolds numbers, which is relevant for the forthcoming heat transfer investigations. Furthermore, the distribution of the wall pressure was determined for different impingement distances and different nozzle mass flow rates. These results indicate a dependency between nozzle mass flow and self induced cross flow between the two opposite plates, which grows up in direction to boundary area of the jet array. Furthermore, the self induced cross flow will be influenced by the impingement plate distance. The higher the nozzle mass flow rate or the smaller the impingement plate distance the higher is the absolute velocity at the boundary area of the plates. This is an striking fact for heat transfer issues at the impingement plate. In this context, preliminary tests have been carried out in the test section of a recirculating free-surface water tunnel. Three subsequent vortex rings were generated periodically at constant *jet to cross flow* velocity ratio of $VR = 4.3$. Frequency, duty cycle and corresponding stroke ratio were varied within the control limited range of the piston cylinder arrangement. The cooling effectiveness was quantified by induced vorticity of the generated vortices at the wall. The ejected mass flux and the relevant time interval of the cooling effect was considered to determine a global measure of actual cooling power. An optimum was found at $Sr_D = 0.30$ and $L/D = 2.4$ representing best-balanced relation between vortex circulation, vortex spacing and applied mass flux. In further steps the dynamic impact on the flow field between the opposite plates due to pulsation of the nozzle jets will be investigated. After the characterization of the dynamic behaviour of the whole impingement jet array, wall heat flux will be considered as well.

Acknowledgement

The authors gratefully acknowledge support by the Deutsche Forschungsgesellschaft (DFG) as part of the collaborative research centre SFB 1029 “Substantial efficiency increase in gas turbines through direct use of coupled unsteady combustion and flow dynamics”.

References

1. Beitelmal, A.H., Saad, M.A., Patel, C.D.: The effect of inclination on the heat transfer between a flat surface and an impinging two-dimensional air jet. Int. J. Heat and Fluid Flow, Vol. 21, pp. 156-163, 2000.

2. Jambunathan, K., Lai, E., Moss, M.A., Button, B.L.: A review of heat transfer data for single circular jet impingement. Int. J. Heat and Fluid Flow, Vol. 13, pp. 106-115, 1992.
3. Martin, H.: Heat and mass transfer between impinging gas jets and solid surfaces. Advances in Heat Transfer 13, pp. 1-60, 1977.
4. Viskanta, R.: Heat transfer to impinging isothermal gas and flame jets. Experimental Thermal and Fluid Science 6, pp. 111-134.
5. Janetzke, T., Nitsche, W., Täge, J.: Experimental investigations of flow field and heat transfer characteristics due to periodically pulsating impinging air jets. Heat and Mass Transfer, 45, 193-206, 2008.
6. Janetzke, T., Nitsche, W.: Time resolved investigations on flow field and quasi wall shear stress of an impingement configuration with pulsating jets by means of high speed PIV and surface hot wire array. Int. J. Heat and Fluid Flow, 30, 877-885, 2009.
7. Janetzke, T.: Experimentelle Untersuchungen zur Effizienssteigerung von Prallkühlkonfigurationen durch dynamische Ringwirbel hoher Amplitude. Dissertation, Technische Universität Berlin. 2010.
8. Pagenkopf, U.: Untersuchung der lokalen konvektiven Transportvorgänge auf Prallflächen. PhD Thesis, Technische Hochschule Darmstadt. 1996.
9. Zumbrunnen, D. A.: Transient convective heat transfer in planar stagnation flows with time-varying surface heat flux and temperature. Journal of Heat Transfer 114, pp. 85-93, 1992.
10. Zumbrunnen, D. A., Aziz, M.: Convective heat transfer enhancement due to intermittency in an impinging jet. Journal of Heat Transfer 115, pp. 91-98, 1993.
11. Sheriff, H., Zumbrunnen, D. A.: Effect of flow pulsations on the cooling effectiveness of an impinging jet. Journal of Heat Transfer 116, pp. 886-895, 1994.
12. Sheriff, H., Zumbrunnen, D. A.: Local instantaneous heat transfer characteristics of arrays of pulsating jets. Journal of Heat Transfer 121, pp. 341-348, 1999.
13. Bräunling, W. J. G.: Flugzeugtriebwerke, 3. Auflage. Springer (1999)
14. Kataoka, K., Suguro, M., Degawa, H., Maruo, K., and Mihata, I.: The effect of surface renewal due to large scale eddies on jet impingement heat transfer. International Journal of Heat and Mass Transfer 30 (3), pp. 559-567, 1987.
15. Sau, R. and Mahesh, K.: Optimization of pulsed jets in cross flow. Journal of Fluid Mechanics 653, pp. 365-390, 2010.
16. Gharib, M. and Rambod, E. and Shariff, K.: A universal time scale for vortex ring formation. Journal of Fluid Mechanics 360, pp. 121-140, 1998.
17. Sau, R. and Mahesh, K.: Dynamics and mixing of vortex rings in cross flow. Journal of Fluid Mechanics 604, pp. 389-409, 2008.